

Ultra-Wideband Antenna with Variable Notch Band Function by Defected Ground Structure and Shorting Pin

Mohammad Akbari^{*1}, Saman Zarbakhsh¹, Reza Movahedinia², and Abdelrazik Sebak²

¹ Young Researchers and Elite Club
Central Tehran Branch, Islamic Azad University, Tehran, Iran
^{*}akbari.telecom@gmail.com, mo_akba@encs.concordia.ca

² Electrical and Computer Department
Concordia University, Quebec, Canada, H3G 1M8

Abstract — In this paper, a simple miniaturized printed antenna for ultra-wideband applications with variable band-notch function is proposed. The presented antenna consists of a square radiating patch and a ground plane with inverted T-shaped slot which increases the bandwidth of 2.3–11 GHz. Frequency band-stop performance is created by two techniques: Defected Ground Structure (DGS) and shorting pins. The designed antenna has a small size of $17 \times 21 \times 1 \text{ mm}^3$ while showing the band rejection performance in the frequency bands of 3.2 to 3.8 and 5.1 to 5.85 GHz, respectively.

Index Terms — Antenna, DGS (Defected Ground Structure), notch band, shorting pin.

I. INTRODUCTION

Commercial ultra-wideband (UWB) systems require compact, cheap antennas with omnidirectional radiation patterns and extended bandwidth [1]. It is a renowned fact that monopole antennas present really appealing physical features, such as simple structure, small size and low cost. Due to all these fascinating characteristics, planar monopoles are quite appealing to be used in emerging UWB applications, and growing research activity is being focused on them. In UWB communication systems, one of major subjects is the design of a small antenna while providing wideband characteristic over the total operating frequency band. Consequently, a big number of microstrip antennas with various structure have been experimentally characterized [2-4]. The frequency range for UWB systems between 3.1 and

10.6 GHz will cause interference to the existing wireless communication systems; as an example, the wireless local area network (WLAN) for IEEE 802.11a operating in 5.15–5.35 GHz and 5.725–5.825 GHz bands, so the UWB antenna with a band-stop performance is needed. To create frequency band-notch function, modified planar monopoles have recently been proposed [5-7]. In [5], novel shape of the slot (folded trapezoid) is used to obtain the appropriated band notched characteristics. Single and multiple half-wavelength U-shaped slots are embedded in the radiation patch to generate single and multiple band-notched [6] functions. In [7], a band-notch function is achieved by using a T-shaped coupled-parasitic element in the ground plane. In this paper, a novel band-notched printed monopole antenna is proposed. The notched bands, covering the 3.2 to 3.8 and 5.1 to 5.85 GHz, is provided by using two techniques: Defected Ground Structure (DGS) and shorting pins. Also by inserting an inverted T-shaped slot on the ground plane, wider impedance bandwidth can be obtained. Measured and simulated results of the constructed miniaturized prototype are presented and discussed.

II. ANTENNA DESIGN

The square monopole antenna is exhibited in Fig. 1, which is printed on a 1 mm thick FR4 substrate with relative permittivity of 4.4. The width W_f of the microstrip feedline is fixed at 1.9 mm. The basic antenna structure consists of a square patch, a feedline, and a ground plane. The square patch has a width W_p . As illustrated in Fig.

1, the patch is connected to a feed line of width W_f and length L_f . On the other side of the substrate, a conducting ground plane of width W_{sub} and length L_{gnd} is placed. The proposed antenna is connected to a 50- Ω SMA connector for signal transmission. The ground plane with an inverted T shape is playing an important role in the broadband characteristics of this antenna, because they can adjust the electromagnetic coupling effects between the patch and the ground plane, and improves its impedance bandwidth without any cost of size or expense [2]. To obtain two notched bands has been used two different techniques, the former DGS (Defected Ground Structure) and the latter shorting pin that will more be examined below.

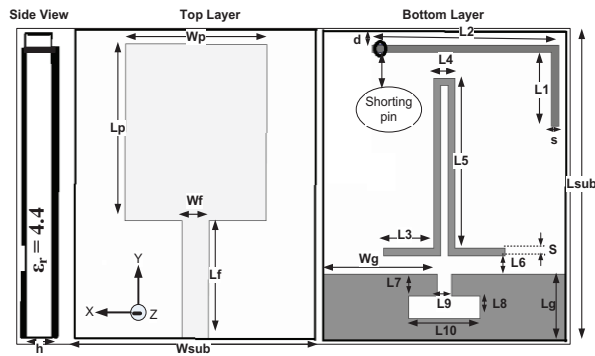


Fig. 1. Geometry of proposed antenna: $W_{sub}=17$, $L_{sub}=21$, $L_p=12$, $W_p=10$, $W_f=1.9$, $L_f=8$, $W_g=8$, $L_g=4.5$, $d=1$, $L_1=3$, $L_2=13$, $L_3=3.5$, $L_4=1.5$, $L_5=11.5$, $L_6=1.25$, $L_7=1.5$, $L_8=1.5$, $L_9=1$, $L_{10}=5$, $S=0.5$, $h=1$, and $\epsilon_r=4.4$.

III. ANTENNA PERFORMANCE AND DISCUSSION

The performance analysis of the proposed antenna is carried out in both frequency- and time-domain.

A. Frequency-domain analysis

In this part, the square monopole antenna with different design parameters were constructed, and the numerical and experimental results of the input impedance and radiation characteristics are presented and discussed. The parameters of this proposed antenna are studied by changing one parameter at a time and fixing the others. Figure 2 depicts the structure of the different square antennas. As illustrated in Fig. 3, bandwidth is increased dramatically and the third resonance has been excited by cutting an inverted T-shaped notch

on the ground. The upper frequency limit of the bandwidth is affected by using a pair of L-shaped arms on the back in a way that the L-shaped arms causes to create a resonance at 11 GHz that extends the bandwidth. However, the main purpose from using a pair of L-shaped arms was to obtain a notch.

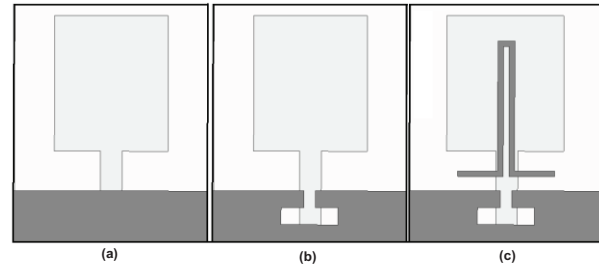


Fig. 2. (a) The ordinary square antenna, (b) the antenna with an inverted T-shape notch on the ground plane, and (c) the antenna with a pair of L-shaped arms on the back (DGS technique).

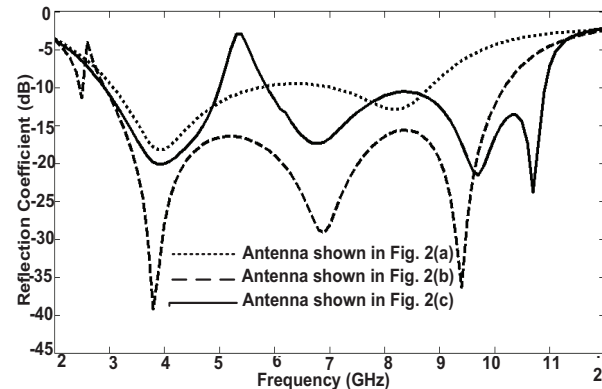


Fig. 3. Simulated reflection coefficient characteristics for the various square monopole antenna structures, as shown in Fig. 2.

In this work, through new technique of DGS and by a pair of L-shaped arms, a band-stop performance at frequency 5.5 GHz is produced that has an acceptable bandwidth. The central frequency of notch can easily be shifted by some key parameters like L_1 . Figure 4 exhibits the different structures of the antenna showing major elements of generating a stop-band, namely a pair of L-shaped arms and shorting pin. Figure 5 demonstrates the voltage standing wave ratio (VSWR) for the three cases shown in Fig. 4. It is quite apparent that the pair of L-shaped arms have effect on notched band at center frequency 5.5 GHz, while shorting pin produces a stop band at center

frequency 3.5 GHz to filter WLAN and WiMAX bands, respectively. Meanwhile, it is found out that both notches are autonomous; i.e., they have no effect on each other. As illustrated in Fig. 6, parameter L5 has a considerable influence on frequency shifting. Increasing the length of L5 results in decreasing the center frequency while the rejection magnitude is nearly constant. A best value L5 for covering 5.15 to 5.825 GHz band corresponds to 11.5 mm. In this study, to generate the band-stop performance on WiMAX band with center frequency 3.5 GHz, we used an arm with length L1+L2 that has been connected to a shorting pin.

The simulated VSWR curves with different values of L1 are plotted in Fig. 7. As shown in Fig. 7, when L1 increases from 1 to 7 mm, the center frequency of the notched band is fallen from 3.8 to 2.8 GHz. Therefore, the optimized L1 is 3 mm. From these results, we can conclude that the notch frequencies are controllable by changing L1 and L5. To understand the behavior of the proposed antenna, Fig. 8 shows simulated current distributions on the radiating patch and a pair of L-shaped arms on the back. It can be observed from Fig. 8 (a), that the current is concentrated on the arms and patch using an arm ended up with shorting pin. It can be noticed that the current direction on the patch is opposed (180 degree phase difference) with the current on arm. On the other hand, Fig. 8 (b) depicts the current distribution at 3.5 GHz. It is clear that most of the current is seen on the pair of L-shaped arms with the current directions on the arms are in opposite direction with the current on patch.

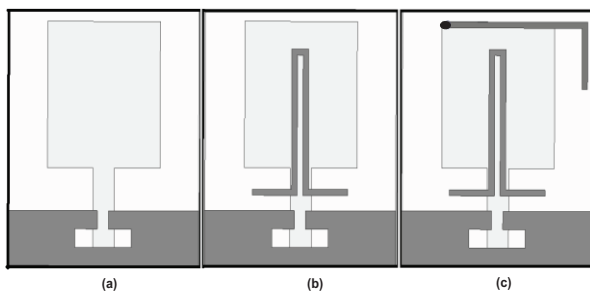


Fig. 4. (a) The square antenna with an inverted T-shaped slot, (b) the square antenna with a pair of L-shaped arms, and (c) proposed antenna.

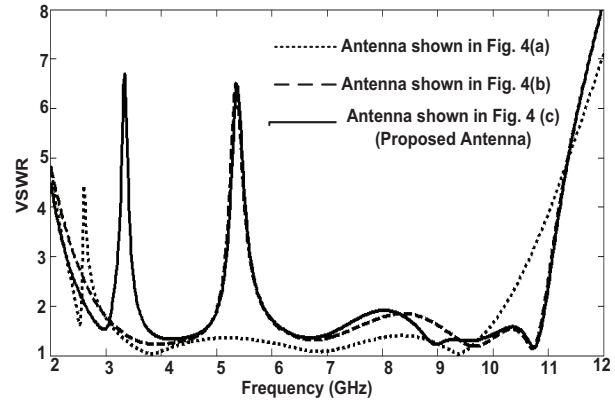


Fig. 5. Simulated VSWR characteristics for antennas shown in Fig. 4.

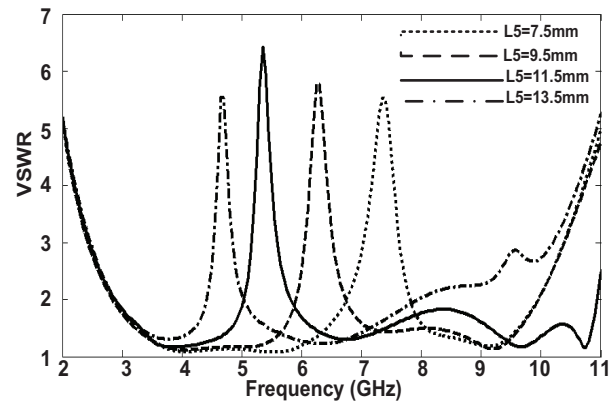


Fig. 6. Simulated VSWR characteristics of the antenna with a pair of L-shaped arms with different values of L5.

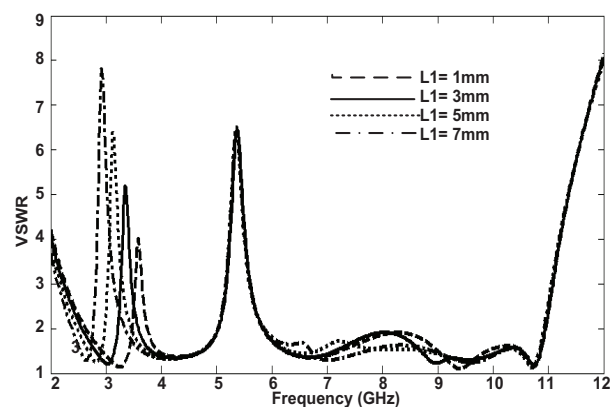


Fig. 7. Simulated VSWR characteristics of the antenna with an arm ended up shorting pin with different values of L1.

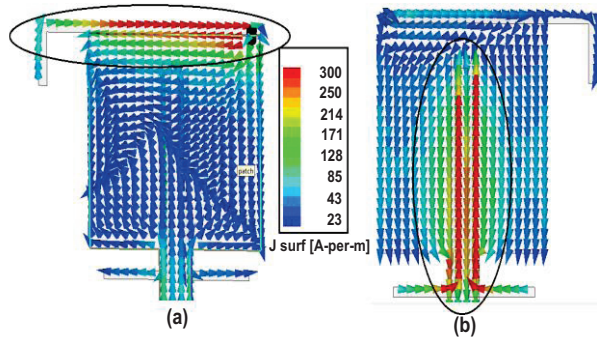


Fig. 8. Simulated surface current distributions on radiating patch: (a) on L-shaped arm ended up shorting pin at 5.5 GHz (bottom view), and (b) on a pair of L-shaped arms at 3.5 GHz (top view).

The proposed antenna with optimal design, as shown in Fig. 9, was fabricated and tested in the Antenna Measurement Laboratory at Iran Telecommunication Research Center. Figure 10 exhibits the measured and simulated VSWR characteristics of the proposed antenna. The fabricated antenna has the frequency band of 2.3 to over 11 GHz. The designed antenna has a small size of $21 \times 17 \text{ mm}^2$ while showing the band rejection performance in the frequency bands of 3.2 to 3.8 and 5.1 to 5.85 GHz, respectively. The measured and simulated VSWR by both software HFSS [8] and CST [9] are shown in Fig. 10. As shown in Fig. 10, there exists a discrepancy between measured data and the simulated results, and this could be due to the effect of the SMA port.

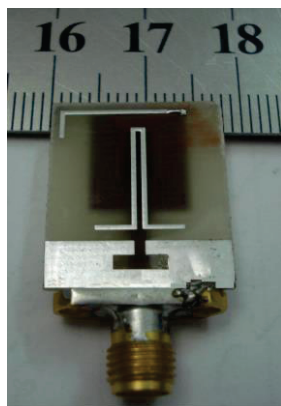


Fig. 9. Photograph of the realized antenna.

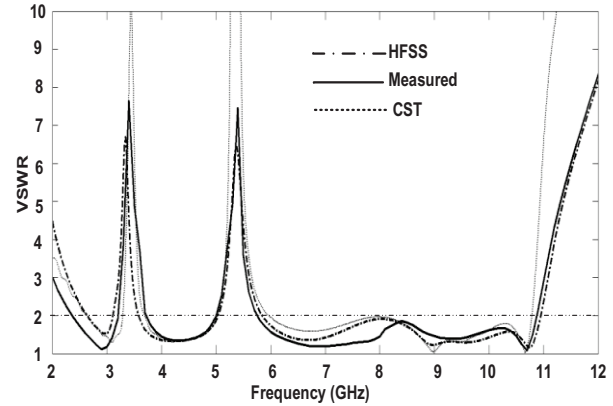


Fig. 10. Measured and simulated VSWR characteristics for the antenna.

Figure 11 illustrates the measured maximum gain of the proposed antenna with and without stop band. A sharp decrease of maximum gain in the notched frequencies band at 3.5 and 5.5 GHz is shown.

For other frequencies outside the notched frequency band, the antenna gain with the slot is similar to those without it. Figure 12 shows the measured radiation patterns including the co-polarization and cross-polarization in the H-plane (x - z plane) and E-plane (y - z plane). It can be seen that the radiation patterns in x - z plane are nearly omnidirectional for the two frequencies while radiation pattern in y - z plane are approximately directional.

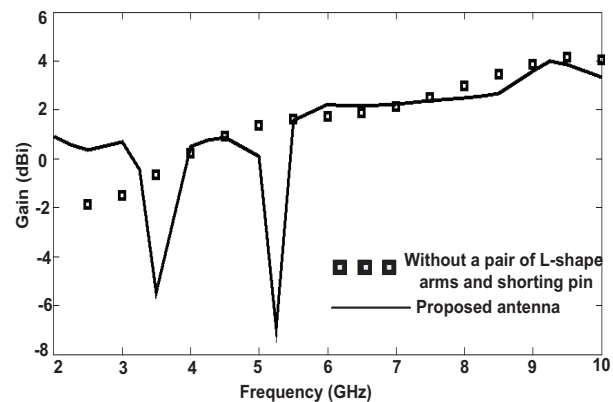


Fig. 11. Measured gain of the antenna without and with stop bands.

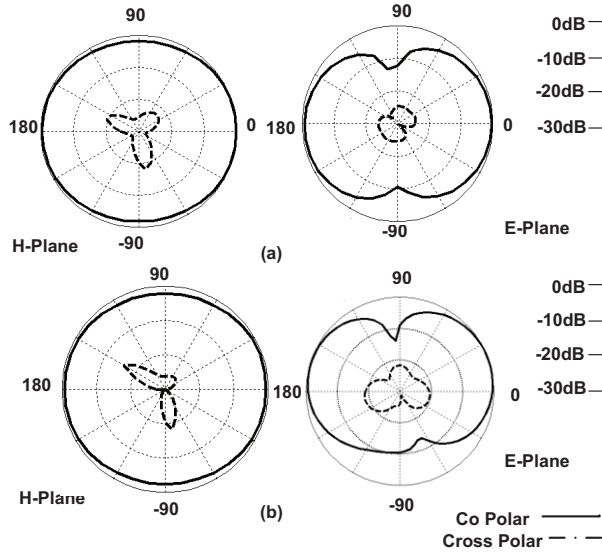


Fig. 12. Measured radiation patterns of the antenna at: (a) 4 and (b) 8 GHz.

B. Time-domain analysis

Computation of the dispersion that happens when the antenna radiates a pulse signal is an important issue in UWB systems. The transmit transfer functions of the antennas were utilized to calculate the radiated pulse in various directions when a reference signal was used at the antenna input. The signal should present an UWB spectrum masking the antenna bandwidth and specially the FCC mask (3.1 up to 10.6 GHz). A pulse of Gaussian seventh derivative is shown in Fig. 13 that is an acceptable approximation to a FCC mask compliant pulse. This pulse is represented in the time domain by:

$$G(t) = A \cdot \exp\left(\frac{-t^2}{2\delta^2}\right), \quad (1)$$

$$G^n(t) = \frac{d^n G}{dt^n} = (-1)^n \frac{1}{(\sqrt{2}\delta)^2} \cdot H_n\left(\frac{t}{\sqrt{2}\delta}\right) \cdot G(t), \quad (2)$$

where, for $n=7$,

$$H_7(t) = 128t^7 - 1344t^5 + 3360t^3 - 1680t. \quad (3)$$

Both signal and spectrum are depicted in Fig. 13. The pulse bandwidth fits very well into the desired mask. Fortunately, after drawing various Gaussian pulses from the first to eighth derivative, it was found that the best pulse to cover the FCC

mask is the seventh derivative. Furthermore, with a few tolerances, the sixth and eighth derivative can be acceptable. The correlation between the transmitted (TX) and received (RX) signals in telecommunications systems, is evaluated using the fidelity factor (4):

$$F = \max_{\tau} \left| \frac{\int_{-\infty}^{+\infty} S(t)r(t-\tau)dt}{\sqrt{\int_{-\infty}^{+\infty} S(t)^2 \cdot \int_{-\infty}^{+\infty} r(t)^2 dt}} \right|. \quad (4)$$

In which $S(t)$ and $r(t)$ are the TX and RX signals, respectively. For impulse radio in UWB communications, it is needful to have a high degree of correlation between the TX and RX signals to avoid losing the modulated information. Although, for most other telecommunication systems, the fidelity parameter is not that relevant. In order to evaluate the pulse transmission characteristics of the antenna without notch, two configurations (side-by-side and face-to-face orientations) were chosen. The transmitting and receiving antennas were placed in a $d=25$ cm distance from each other [10]. As shown in Fig. 14, the received pulses in each of the two orientations are broadened, a relatively good similarity exists between the RX and TX pulses. Using (4), the fidelity factor for the face-to-face and side-by-side configurations was earned equal to 0.95 and 0.96, respectively. These values for the fidelity factor demonstrate which the antenna imposes negligible effects on the transmitted pulses. The pulse transmission results are obtained using CST [9].

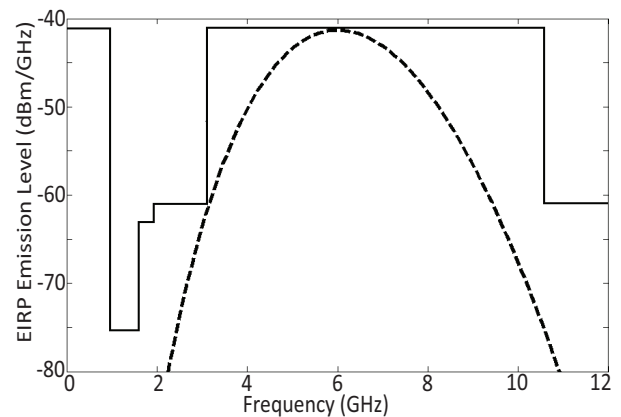


Fig. 13. Power spectrum density compared to FCC mask.

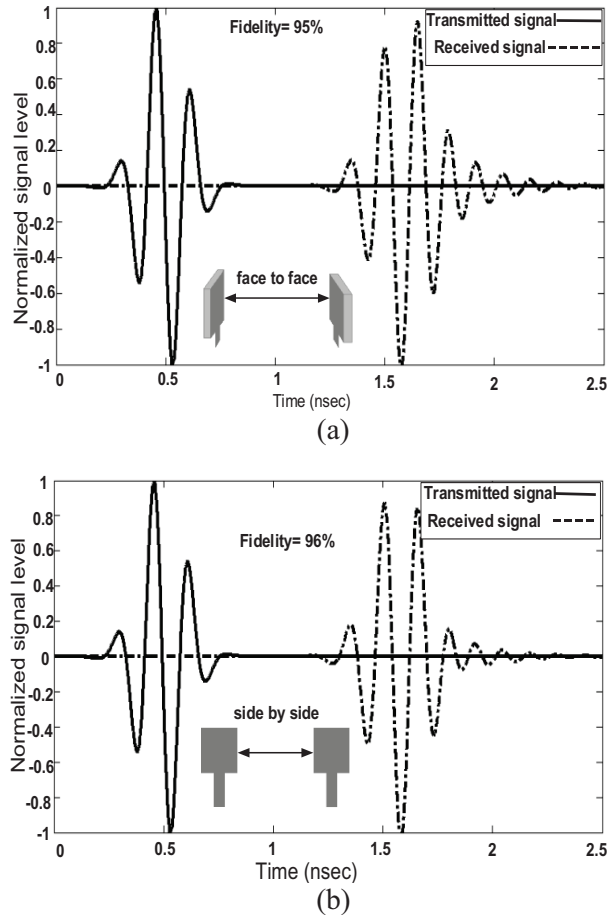


Fig. 14. Transmitted and received pulses in time domain for a UWB link with identical antennas without notches in: (a) face-to-face and (b) side by side orientations.

IV. CONCLUSION

In this paper, a novel microstrip antenna with extended bandwidth capability for UWB applications was presented. In this design, the proposed antenna can operate from 2.3 to 11 GHz with $VSWR < 2$, and displays a good omnidirectional radiation pattern even at higher frequencies. The designed antenna has a small size of $17 \times 21 \text{ mm}^2$ while showing a band rejection performance in the frequency bands of 3.2 to 3.8 and 5.1 to 5.85 GHz, respectively. Good reflection coefficient and radiation pattern characteristics are obtained in the frequency band of interest. Simulated and experimental results exhibit that the antenna could

be a good candidate for UWB application.

REFERENCES

- [1] H. Schantz, *The Art and Science of Ultra Wideband Antennas*, Artech House, Norwood, MA, 2005.
- [2] M. Akbari, M. Koohestani, Ch. Ghobadi, and J. Nourinia, "Compact CPW-fed printed monopole antenna with super wideband performance," *Microwave Opt. Technol. Lett.*, 53, pp. 1481-1483, July 2011.
- [3] M. Akbari, M. Koohestani, Ch. Ghobadi, and J. Nourinia, "A new compact planar UWB monopole antenna," *International Journal of RF and Microwave Computer-Aided Engineering*, 21, pp. 216-220, 2011.
- [4] M. Mighani, M. Akbari, and N. Felegari, "Design of a small rhombic monopole antenna with parasitic rectangle into slot of the feed line for SWB application," *The Applied Computational Electromagnetics Society*, 27, pp. 74-79, 2012.
- [5] M. Ojaroudi, "Printed monopole antenna with a novel band-notched folded trapezoid ultra-wideband," *J. Electromagn. Waves. Appl.*, 23, pp. 2513-2522, 2009.
- [6] M. Ojaroudi, Gh. Ghanbari, N. Ojaroudi, and Ch. Ghobadi, "Small square monopole antenna for UWB applications with variable frequency band-notch function," *IEEE Antennas Wirel. Propag. Lett.*, 8, pp. 1061-1064, 2009.
- [7] R. Rouhi, Ch. Ghobadi, J. Nourinia, and M. Ojaroudi, "Ultra-wideband small square monopole antenna with band notched function," *Microwave Opt. Technol. Lett.*, 52, pp. 2065-2069, 2010.
- [8] Ansoft High Frequency Structure Simulation (HFSS), ver. 10, Ansoft Corporation, Pittsburgh, PA, 2005.
- [9] CST Microwave Studio, ver. 2008, Computer Simulation Technology, Framingham, MA, 2008.
- [10] C. R. Medeiros, J. R. Costa, and C. A. Fernandes, "Compact tapered slot UWB antenna with WLAN band rejection," *IEEE Antennas and Wireless Propagation Letters*, vol. 8, pp. 661-664, 2009.